SSCL-573

SSCL-573

Superconducting Super Collider Laboratory

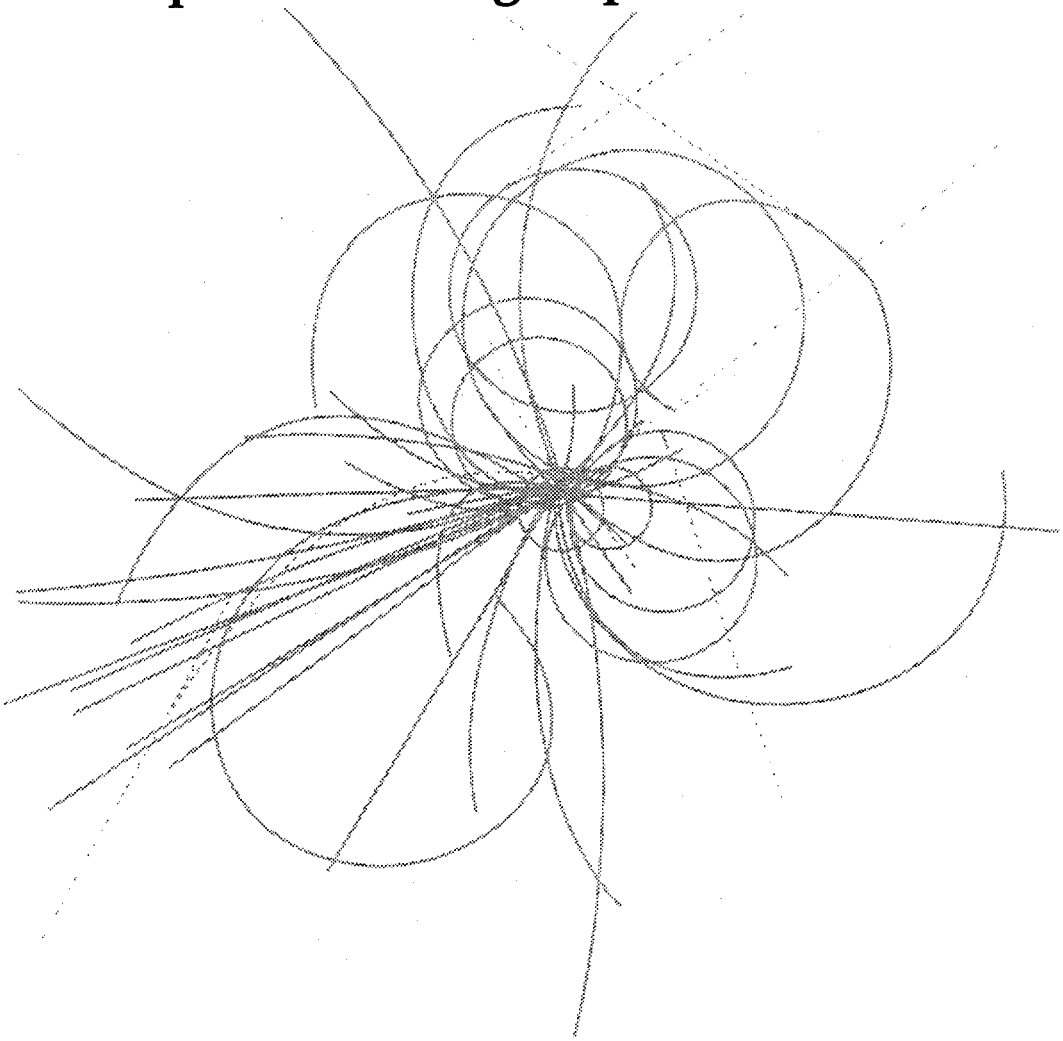

Measurement of AC Electrical Characteristics of SSC Dipole Magnets at Brookhaven

K. Smedley

April 1992

SSCL-573

Measurement of AC Electrical Characteristics of SSC Dipole Magnets at Brookhaven

K. Smedley

Superconducting Super Collider Laboratory*
2550 Beckleymeade Avenue
Dallas, Texas 75237

April 1992

* Operated by the Universities Research Association, Inc., for the U.S. Department of Energy under Contract No. DE-AC35-89ER40486.

1.0 INTRODUCTION

The SSC collider is designed to have circumference of 87 km. The superconducting magnets along the collider ring are grouped into ten sectors. Each sector, a string of average length of 8.7 km, is powered by one power source located near the center of the sector. Because of the alternating-current (ac) electrical characteristics of the magnets, the power supply ripple currents and transients form a time and space distribution in the magnet string which affects particle motions. Additionally, since the power supply load is a magnet string, the current regulation loop design is highly dependent upon the ac electrical characteristics of the magnets.

A means is needed to accurately determine the ac electrical characteristics of the superconducting magnets. The ac characteristics of magnets will be used to predict the ripple distribution of the long string of superconducting magnets. Magnet ac characteristics can also provide necessary information for the regulation loop design.

This paper presents a method for measuring the ac characteristics of superconducting magnets. Two collider dipole magnets, one superconducting and one at room temperature, were tested at Brookhaven National Lab.

2.0 MEASUREMENT METHOD

Figure 1 shows the cross section of a typical superconducting dipole magnet. The major magnet components include a copper-coated beam tube of radius a, a coil of average radius b, four heater strips, a laminated aluminum collar, a laminated iron yoke, and a cryogenic shell. When the temperature is below 4.2 K, the direct-current (dc) resistivity of the coil disappears; therefore, the magnet behaves like a pure inductor at low frequencies. If the magnet current contains ac components, however, it will induce eddy currents in the beam tube, magnet coil, and other metallic components;[1] the magnet will show some resistivity. A resonance at high-frequency range may occur between the magnet inductance and capacitance of the coil to ground and turn-to-turn. The ac electrical characteristics of the magnet are therefore frequency dependent.

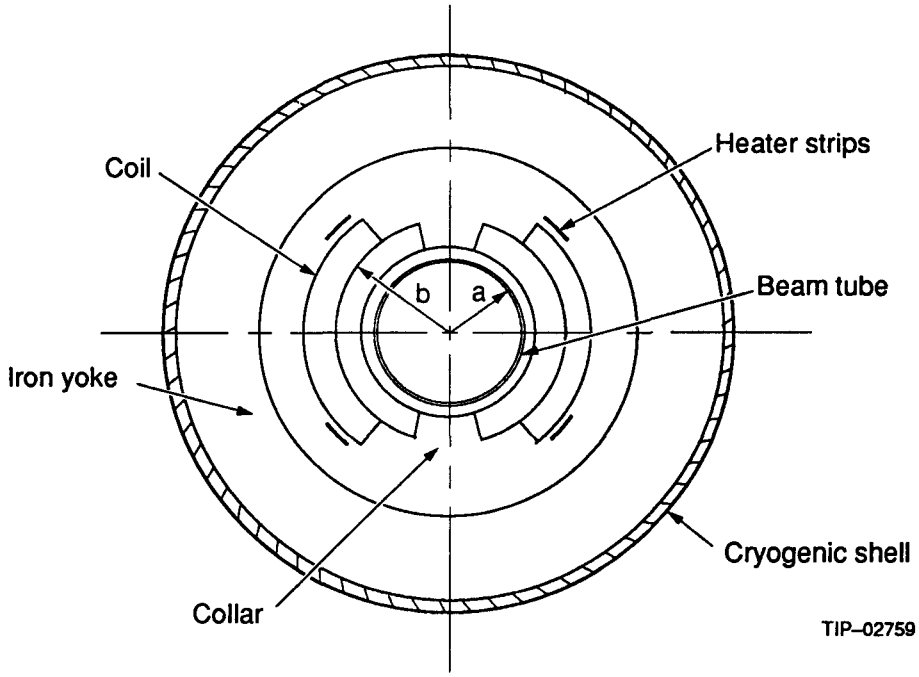

Figure 1. Cross Section of Superconducting Dipole Magnet.

2.1 Magnet Equivalent Circuit

The beam tube eddy current phenomenon can be analyzed by a coupled inductor circuit shown in Figure 2. Primary inductor L_1 represents the n-turn superconducting coil, secondary inductor L_2 represents the one-turn eddy current path in the beam tube, and R_b represents the beam tube resistance. Suppose the mutual inductance is M and the coupling coefficient is $\sqrt{k} = \frac{M}{\sqrt{L_1 L_2}}$. The circuit equations are derived as follows:

$$v_1 = j\omega L_1 i_1 - j\omega M i_2 \ , \tag{1}$$

$$R_b i_2 = j\omega M i_1 - j\omega L_2 i_2 \ . \tag{2}$$

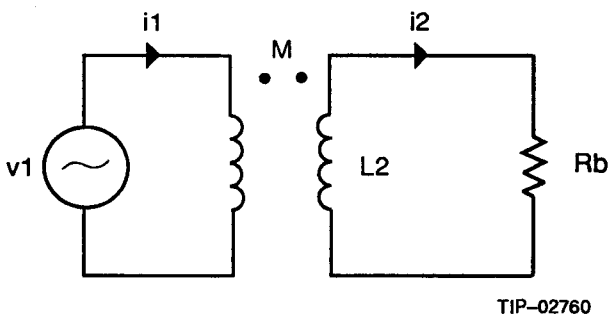

Figure 2. Eddy Current Circuit.

The voltage and current relationship of the primary winding are found from the circuit equations:

$$i_2 = \frac{j\omega M}{R_b + j\omega L_2} i_1 \ , \tag{3}$$

$$v_1 = j\omega L_1 i_1 - j\omega M \frac{j\omega M}{R_b + j\omega L_2} i_1 \ . \tag{4}$$

The impedance of the magnet is therefore obtained as

$$z = \frac{v_1}{i_1} \tag{5}$$

$$= j\omega L_1 - j\omega M \frac{j\omega M}{R_b + j\omega L_2} \ . \tag{6}$$

With some reorganizing, the impedance expression becomes

$$z = j\omega L_1 - \frac{j\omega M(j\omega M + \frac{R_b M}{L_2} - \frac{R_b M}{L_2})}{R_b + j\omega L_2} \tag{7}$$

$$= j\omega L_1 (1 - \frac{M^2}{L_1 L_2}) + \frac{j\omega \frac{M^2}{L_1 L_2} L_1 R_b}{R_b + j\omega L_2} \ . \tag{8}$$

Let $L_2 = \frac{kL}{n^2}$ and $R = n^2 R_b$, the impedance function is simplified.

$$z = j\omega L(1-k) + \frac{j\omega k L R}{R + j\omega k L} \ . \tag{9}$$

An equivalent circuit shown in Figure 3 is obtained from the preceding impedance function. The Laplace form of the impedance is

$$z = \frac{sL\left(1 + \frac{s}{R/(k(1-k)L)}\right)}{1 + \frac{s}{R/(kL)}} \ . \tag{10}$$

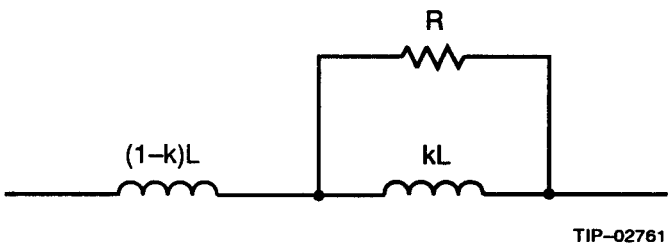

Figure 3. Equivalent Circuit.

Further, with the capacitance between each turn and capacitance between the coil and the ground taken into account, the equivalent circuit is modified to form a circuit model as shown in Figure 4. The Laplace form impedance is

$$z \approx \frac{sL\left(1 + \frac{s}{R/(k(1-k)L)}\right)}{(1 + \frac{s}{R/(kL)})\left(1 + \frac{RC}{4}s + (1-k)\frac{LC}{4}s^2\right)} \ . \tag{11}$$

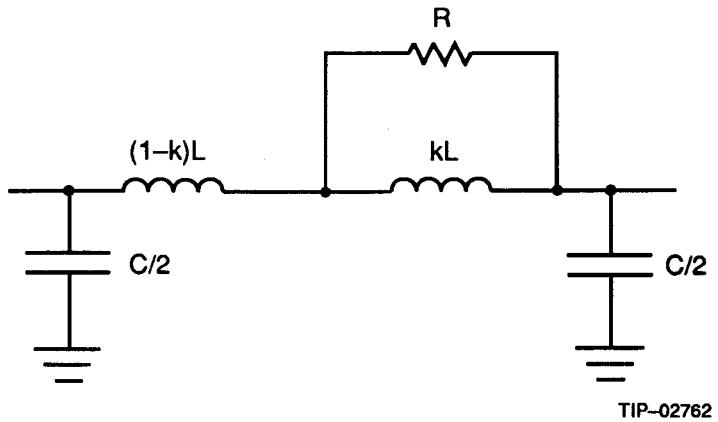

Figure 4. Impedance Model.

2.2 Impedance Measurement

An HP network analyzer (HP 3563A) produces a swept frequency signal in the frequency range of interest, *e.g.*, 0.1 Hz to 10 kHz. A Kepco power amplifier (BOP 36-12M) boosts the current level (maximum 10 V, 10 A) of the swept signal for high measurement precision. The input voltage v, across the magnet terminals, and the input current i through the external 1Ω resistor are measured by the network analyzer to generate the impedance transfer function. Figure 5 shows the series impedance measurement circuit. To measure the shunt impedance between the magnet and the ground, two terminals of the magnet are shorted. Figure 6 shows the shunt impedance measurement circuit. The measurement data is a frequency response trace. Curve fitting techniques are used to derive a linear system model from the measurement data. The pole/zero model is developed by calculating the least-squares fit of the frequency response data to the linear system model. The model will have a form of:

$$z = \frac{As(1 + s/\omega_2)}{(1 + s/\omega_1)\left(1 + s/Q\omega_3 + s^2/(\omega_3^2)\right)} . \tag{12}$$

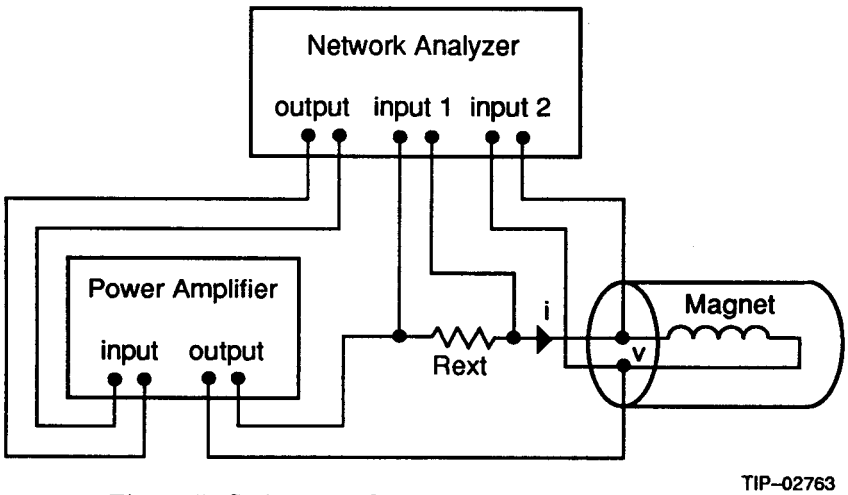

Figure 5. Series Impedance Measurement Circuit.

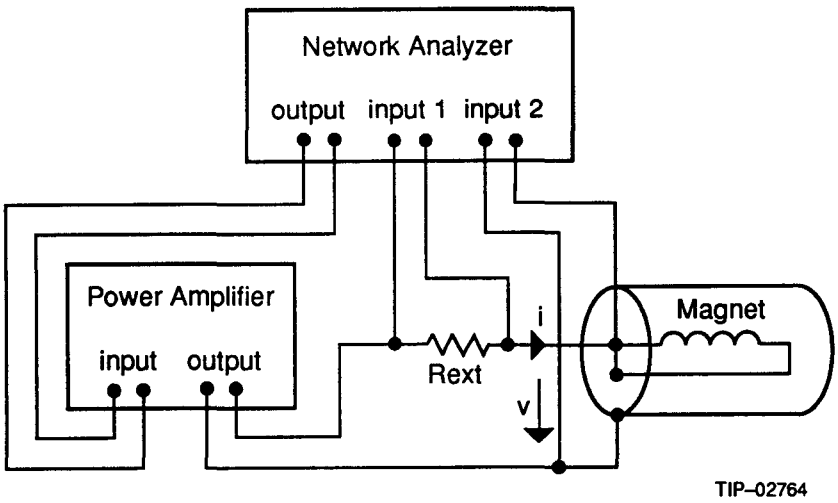

Figure 6. Shunt Impedance Measurement Circuit.

Comparing the predicted impedance function in Eq. (11) and the measured impedance function in Eq. (12), the circuit parameter L, R, k and C can be determined:

$$L = A \ , \tag{13}$$

$$\frac{R}{k(1-k)L} = \omega_2 \ , \tag{14}$$

$$\frac{R}{kL} = \omega_1 \ , \tag{15}$$

$$\frac{2}{\sqrt{(1-k)LC}} = \omega_3 \ . \tag{16}$$

Often, the measured impedance transfer function may have some additional poles and zeros to the predicted impedance transfer function; therefore, proper adjustments, according to the understanding of the magnet physics, to the model may be necessary. The magnet tests done at Brookhaven National Lab serve as a good example to understand the measurement technique.

3.0 BROOKHAVEN MAGNET TESTS

A pair of 50-mm aperture, 15-m-long superconducting dipole magnets, twin magnets DCA 207 and DCA 208, were tested in Brookhaven National Lab Jan 27–28, 1992. One magnet was superconducting, the other was at room temperature.

DCA 207 is tested at room temperature. Figures 7 and 8 show the series and shunt impedance, respectively, of warm dipole DCA 207. The measurement data shows that warm dipole DCA 207 has a dc resistance of 5.77 Ω and dc inductance of 70.7 mH. The shunt capacitance between the coil and ground is 278 nF, when the heater strips are floating. The shunt capacitance becomes 306 nF when the heat strips are shorted to ground.

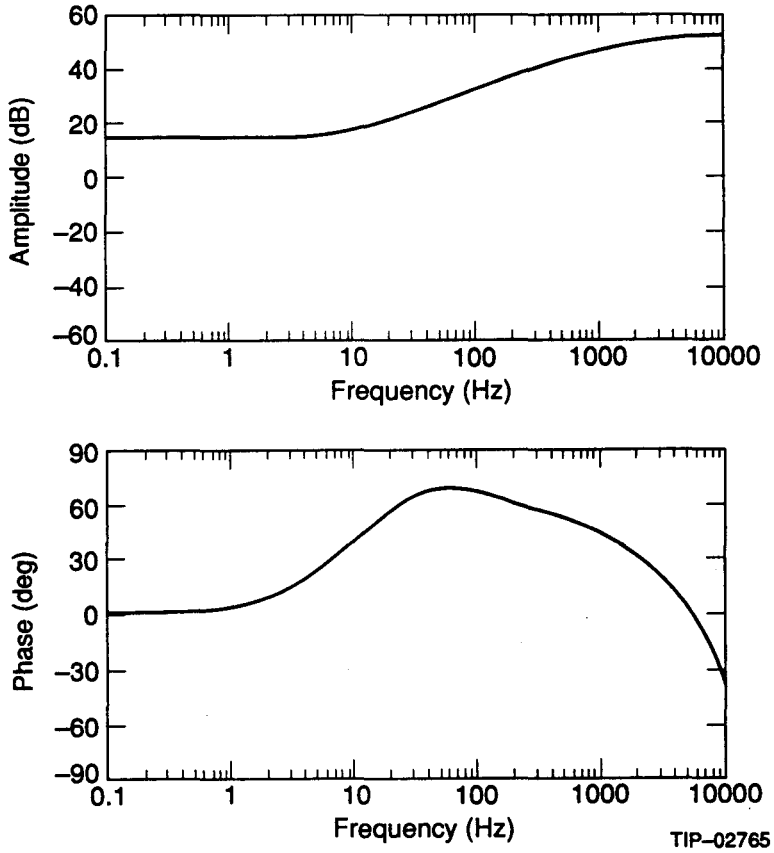

Figure 7. Series Impedance of Warm Dipole DCA 207.

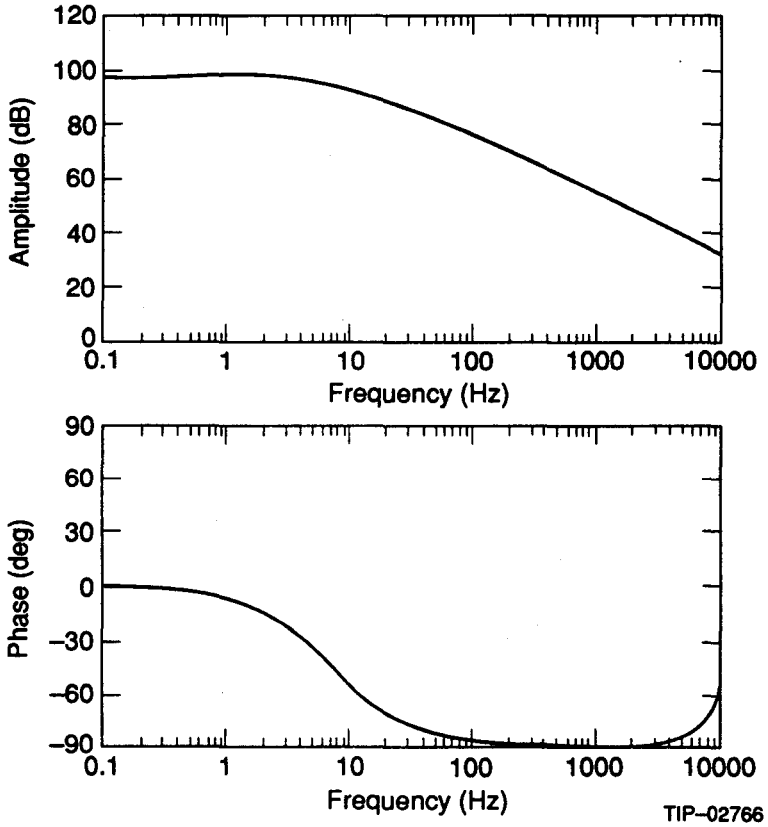

Figure 8. Shunt Impedance of Warm Dipole DCA 207.

Dipole DCA 208 is tested at 4.2 K. Figures 9 and 10 show the series and shunt impedance, respectively, of the cold dipole DCA 208. The cold magnet DCA 208 has a dc inductance of 65.7 mH. The shunt capacitance between the coil and the ground is 898 nF with the heat strips grounded.[2] This unusually larger value of the capacitance may be due the external circuitry. A transfer function impedance model is derived from the cold dipole DCA 208 measurement data by curve-fitting:

$$z = \frac{0.0657s(1+\frac{s}{2\pi 48})(1+\frac{s}{2\pi 588})(1+\frac{s}{2\pi 9723}+\frac{s^2}{(2\pi 13324)^2})}{(1+\frac{s}{2\pi 38})(1+\frac{s}{2\pi 287})(1+\frac{s}{2\pi 1338}+\frac{s^2}{(2\pi 2025)^2})(1+\frac{s}{2\pi 6743})} . \tag{17}$$

The curve-fitting impedance function indicates some unexpected poles and zeros to the predicted transfer function. The measured trace and the trace generated by curve-fitting model are plotted in Figure 11.

The curve-fitted model is a very good approximation of the real system. However, the model gets very complicated. Since the system frequency bandwidth of the magnet string is below 1 kHz, the pole at 6.7 kHz and zeros at 13 kHz are neglected. The impedance circuit model is adjusted as

$$z = \frac{0.0657s(1+\frac{s}{2\pi 48})(1+\frac{s}{2\pi 588})}{(1+\frac{s}{2\pi 38})(1+\frac{s}{2\pi 287})(1+\frac{s}{2\pi 1338}+\frac{s^2}{(2\pi 2025)^2})} . \tag{18}$$

The model described in Eq. (18) is synthesized to a circuit shown in Figure 12. The existence of the additional pole at 38 Hz and the additional zero at 48 Hz might be due to some eddy current in the collar or the iron yoke. This model matches the measured data very closely at low frequencies. However, some discrepancies in high frequency are introduced by dropping the high frequency pole and zeros. The measured trace and the trace generated by the adjusted model are plotted in Figure 13. The parameters are calculated from the transfer function:

$$L = 65.6\,\mathrm{mH} , \tag{19}$$

$$R = 273.5\,\Omega , \tag{20}$$

$$k_1 = 0.207 , \tag{21}$$

$$R_1 = 3.3\,\Omega , \tag{22}$$

$$k_2 = 0.317 , \tag{23}$$

$$R_2 = 45.6\,\Omega , \tag{24}$$

$$C1 = 74\,\mathrm{nF} , \tag{25}$$

$$C = 898\,\mathrm{nF} . \tag{26}$$

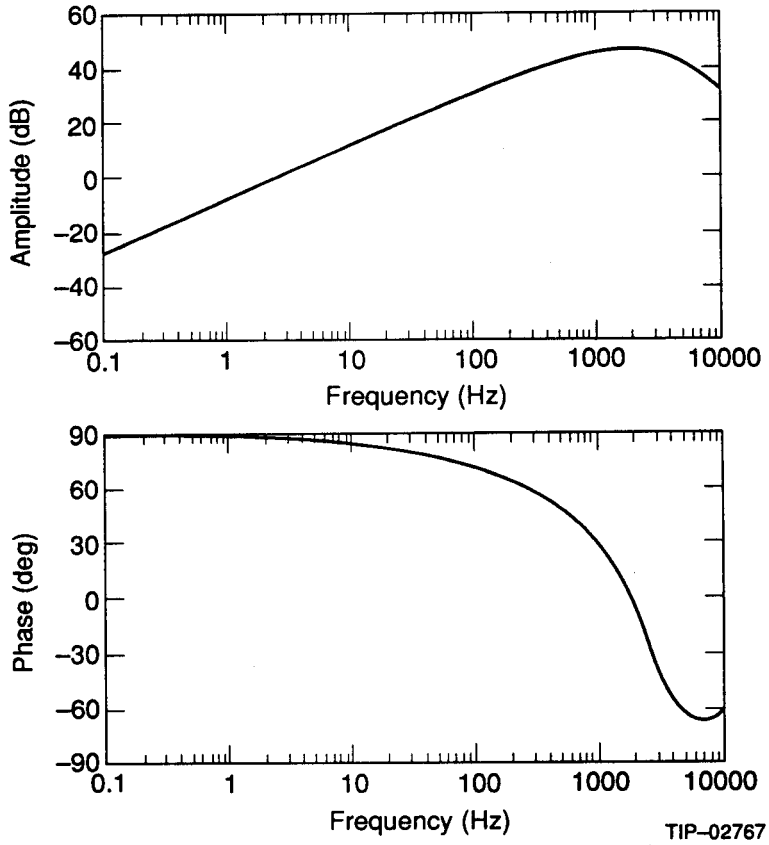

Figure 9. Series Impedance of Cold Dipole DCA 208.

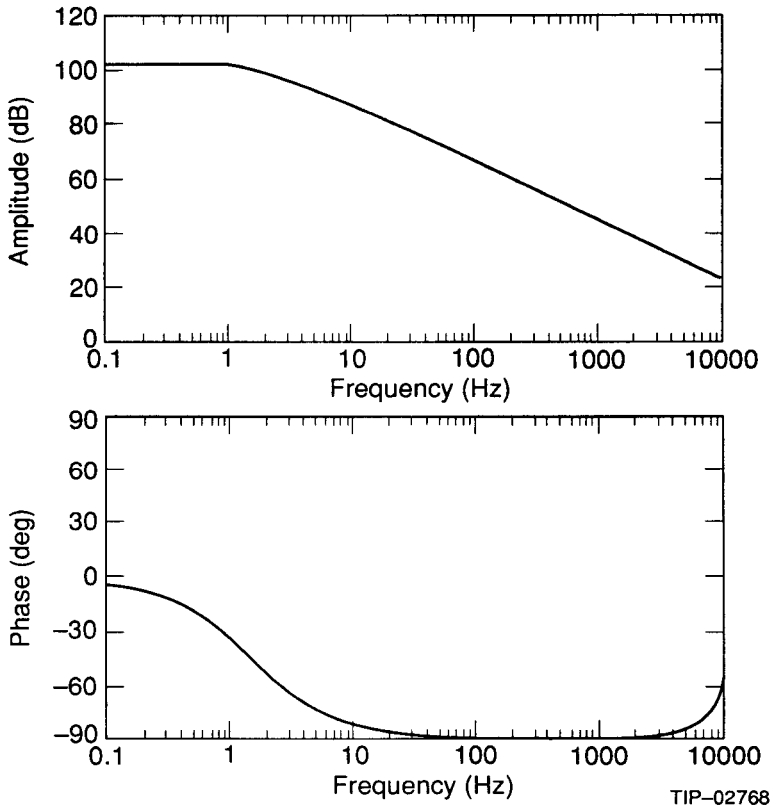

Figure 10. Shunt Impedance of Cold Dipole DCA 208.

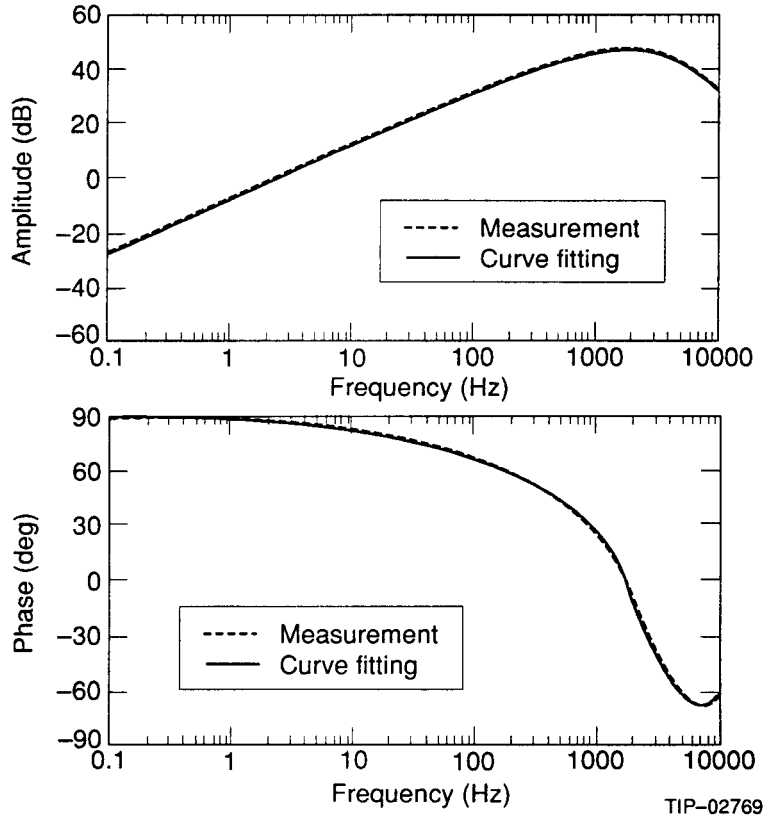

Figure 11. Curve Fitting to the Measured Impedance Data of Cold Dipole DCA 208.

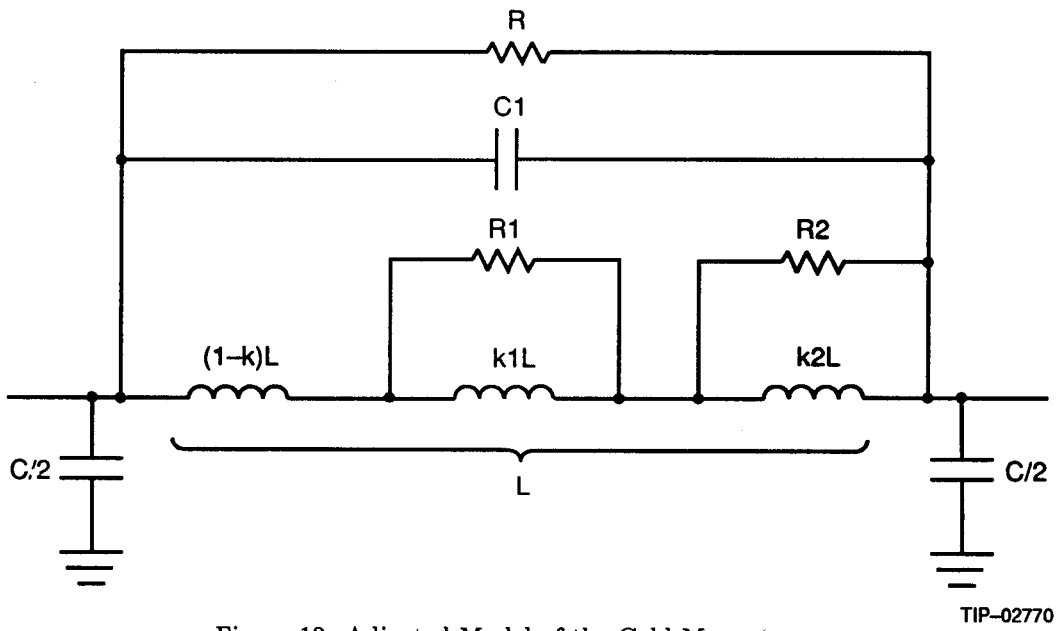

Figure 12. Adjusted Model of the Cold Magnet.

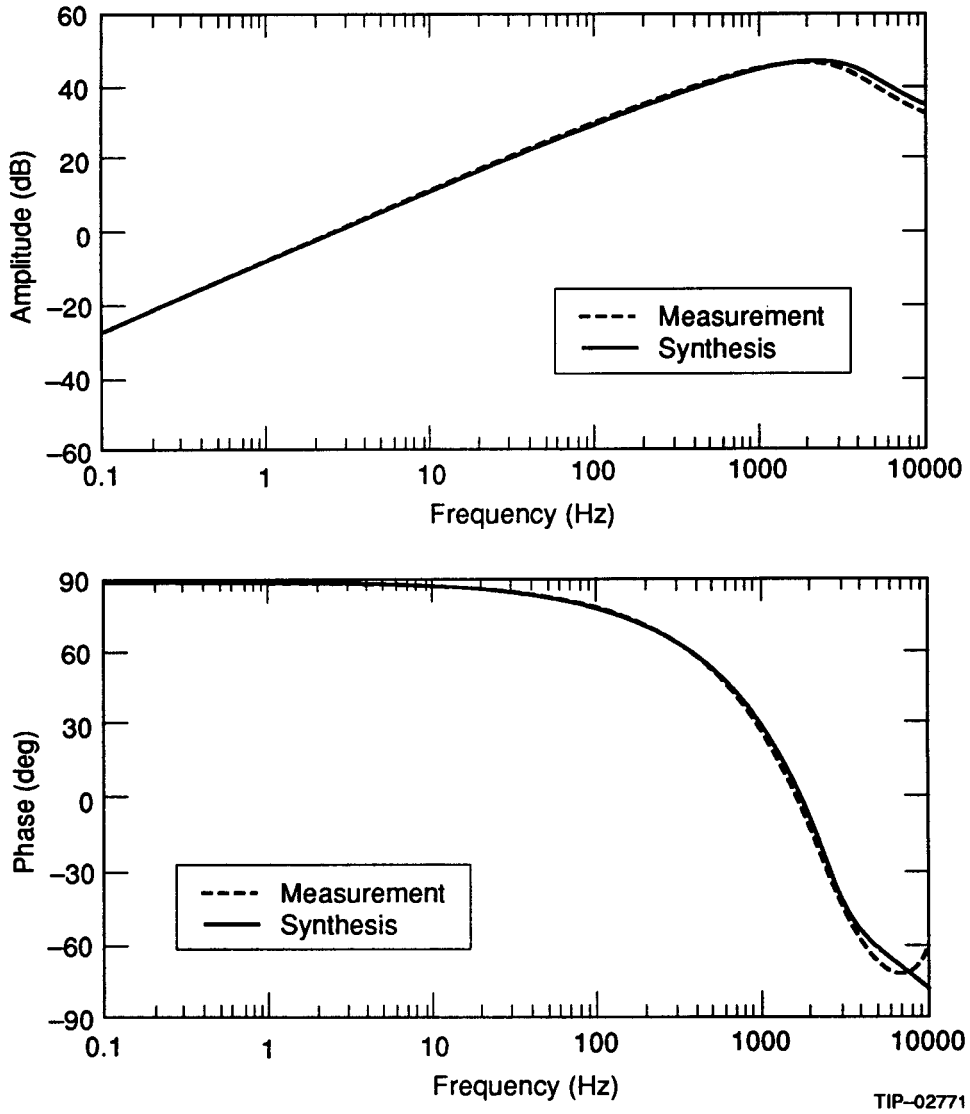

Figure 13. Adjusted Curve Fitting to the Measured Impedance Data of Cold Dipole DCA 208.

The measured shunt capacitance of the cold magnet DCA 208 is significantly larger than that of the warm magnet DCA 207. Measurement of the same magnet, DCA 208, under room temperature conditions is necessary for a better comparison.

4.0 SUMMARY

The frequency dependent ac electrical characteristics are measured by the network analyzer. A curve fitting technique indicates the transfer function of the magnet impedance from the measured data. The electrical circuit model is obtained from synthesis of the transfer function. The circuit model shows the magnet inductance, eddy current resistance, and intra-coil and coil-to-ground capacitance. The measurement method shows high accuracy, excellent repeatability, and ease of use.

ACKNOWLEDGEMENTS

The author would like to thank Al Mendoza for his contribution in the experiments. Credit is also due to the staff members in Accelerator Detector Department of Brookhaven National Lab for their support.

REFERENCES

1. R. Shafer, "Eddy Current, Dispersion Relations, and Transient Effects in Superconducting Magnets," Fermi Lab. report, TM-991, 1980, see also IEEE Transaction on Magnets, Vol. **MAG-17**, **NO.1**, January 1981.
2. George Ganetrs, private communication.